ANALYSIS OF VASCULAR FLOWS WITH OPTICAL TECHNIQUES

V.R. PALERO[c], E.M. ROCHE, L. ARÉVALO, M. NICOLÁS, M. MALVÈ, M.A. MARTÍNEZ, M.P. ARROYO

Aragón Institute of Engineering Research (I3A), University of Zaragoza, Zaragoza, Spain

[c]Corresponding author: Tel.: +34976762691; Fax: +34976761233; Email: palero@unizar.es

KEYWORDS:
Main subjects: fluid-wall interaction, flow visualization
Fluid: biological flows
Visualization method(s): PIV, digital holography
Other keywords: brain aneurisms, atheroma, antithrombotic filter

ABSTRACT: Cardiovascular diseases (CVD) are the main cause of life lost in developed countries and one of the main causes of disability in the population. The simultaneous measurement of the velocity field (3D-3C measurement) and of the vessel shape and deformation would allow the study of the fluid-wall interaction which provides the wall shear stress, one of the most important parameters in the development of these diseases. Two set of experiments were carried out. In the first set, the velocity field in a spherical brain aneurism model made of silicone is analyzed using high speed PIV and digital image plane holography, in order to obtain the 2D-3C velocity field. The PIV images provide the in-plane velocity components. The phase maps obtained from the holograms provide information not only on the out-of-plane component but also about the deformation produced in the model wall. In another set of experiments, the influence of a prototype of antithrombotic filter for vena cava is evaluated. A numerical model is being developed, which will use these experimental data for validating the code.

INTRODUCTION

Cardiovascular diseases (CVD) are the main cause of life lost in developed countries and one of the main causes of disability in the population. Vascular diseases as brain aneurysms or pulmonary thrombotic embolism (PTE) are serious diseases, very frequent and of different treatment, being one of the first causes of death in Europe.

A brain aneurysm, also called cerebral or intracranial aneurysm, is an abnormal dilatation of one of the arteries in the brain [1]. Before an aneurysm ruptures, patients often experience no symptoms, so the aneurysms are often discovered when they rupture, causing bleeding into the brain or the space closely surrounding the brain called the subarachnoid space. A subarachnoid haemorrhage from a ruptured brain aneurysm can lead to a hemorrhagic stroke, brain damage and death.

Despite recent advances in surgical techniques and therapies, PTE is still a serious disease. Anticoagulant therapy and fibrinolisis are medical treatments for hard cases for PTE. In case anticoagulation was not sufficient to save the patient life, traditionally the only possible treatment was the blocking of the blood flow in the vena cava inferior. This procedure was performed firstly in chirurgical set-up and then through filter [2, 3]. Filters for vena cava are usually made of steel or alloy of titanium and nickel. Generally, these antithrombotic filters are conical devices single or double baskets with a head vertex and anchoring barbs along of each straight struts. These present a space left in the middle in order to retain thrombi which are bigger than a fixed maximal dimension. The retained thrombi, which diameter can reach 3mm are solved by the fibrinolitic endogen system.

Some problems may arise when the filter is implanted. Anchoring barbs can damage endothelial tissue of the arterial wall with associated clinical complications. Filter migration is another associated risk of implantation. Also, the filter should retain all big-size thrombi but it is not clear if medium or small-size thrombi have to be retained as well. Moreover, the clinical implications of this are not clear. Lastly, filter obstruction due to thrombi retaining is also a possible problem [3, 4].

Thus, it is important to develop new numerical tools in order to design new types of filters. The filter should maximize the dimension and the number of retained thrombi without migration problems. It should also minimize possible arterial wall injuries or fibrosis. These numerical tools have to be validated with experimental results obtained from measuring the velocity field in a simulated vein with an antithrombotic filter inside.

In this work, experiments in two different vessels have been carried out. First, the velocity field in a spherical brain aneurism model made of silicone is analyzed using high speed PIV and digital image plane holography, in order to obtain the 2D-3C velocity field. The in-plane velocity components are measured with PIV, while the out-of-plane component is obtained from the difference phase maps obtained from the digital holograms. Second, the influence of a prototype of antithrombotic filter for vena cava is evaluated. The velocity field measured with PIV in a vein model with a filter inside is compared with the preliminary results obtained with a new numerical model which is under development.

FUNDAMENTALS OF THE MEASUREMENT TECHNIQUES Particle image velocimetry (PIV) is a well known technique for the measurement of the in-plane velocity components in a seeded fluid plane (2D- 2C technique) illuminated with a laser sheet. The analysis of consecutive recordings of the fluid plane, taken at known time intervals (ΔTPIV) provides the whole velocity field in such plane. [5]

In Digital Image Plane Holography (DIPH), a fluid plane is illuminated with a laser sheet as in PIV. A lens is used to form its image in a camera sensor where it interferes with a reference wave, making a so-called image hologram. The reference wave can be a collimated wave [6], which allows an easy reconstruction of the hologram. However, in this work a divergent reference beam, whose source is located at the same distance from the sensor as the imaging lens aperture, is used [7, 8, 9]. This holographic set-up produces a lensless Fourier transform hologram of the lens aperture and allows an easy isolation of the real image term from the virtual image and dc terms. If $\tilde{o} = o e^{i\varphi_o}$ is the light scattered by the object and $\tilde{r} = r e^{i\varphi_r}$ is the reference beam, the hologram intensity can be written as:

$$I = o^2 + r^2 + roe^{i(\varphi_o - \varphi_r)} + roe^{-i(\varphi_o - \varphi_r)} \qquad (1)$$

In the spatial domain these four terms are mixed, but they can be separated in the frequency domain using the appropriated reference beam.

In the reconstruction process [7] the real image of the lens aperture is selected, while the rest is blocked. Then, the complex amplitude distribution is propagated to the object plane, where the intensity and phase distributions are reconstructed. The out-of-plane component can be extracted from subtracting two phase distributions, separated a time interval ΔT, using an interferometric analysis.

The PIV analysis for the measurement of the in-plane velocity components is well known and can be found in many works [5]. The interferometric analysis for getting the out-of-plane component is known [10] and only but a brief reminder is presented in the following.

When two holograms are recorded within a time interval ΔT, the intensity distribution on the sensor plane for each of them can be written as:

$$\begin{aligned} I_A &= o_A^2 + r^2 + 2o_A r\cos(\varphi_{oA} - \varphi_r) \\ I_B &= o_B^2 + r^2 + 2o_B r\cos(\varphi_{oB} - \varphi_r) \end{aligned} \qquad (2)$$

where the amplitude and phase of the reference are considered constant. As the object is a particle image field, the phase is a spatially random magnitude. However, the difference is not and it is related with the local displacement $\vec{L}$ as:

$$\Delta\varphi = (\vec{k}_o - \vec{k}_i)\vec{L} = \vec{K}\cdot\vec{L} = \vec{K}\cdot\vec{V}\Delta T \qquad (3)$$

The vector $\vec{K}$ is the so-called sensitivity vector, which is the difference between the observation ($\overrightarrow{k_o}$) and the illumination ($\overrightarrow{k_i}$) vectors. The illumination vector is a vector in the direction of the propagation of the illumination beam, and is given by $\overrightarrow{k_i} = -\frac{2\pi}{\lambda}\hat{j}$ as in the present case the fluid illumination is done from the top. The observation vector depends on the direction of visualization. Depending on the sensor size and the magnification, the k_{ox} and k_{oy} components can be neglected and the observation vector can be approximated by $\overrightarrow{k_o} = -\frac{2\pi}{\lambda}\hat{k}$. Then, the phase difference can be expressed as:

$$\Delta\varphi = -\frac{2\pi}{\lambda}(L_y + L_z) \qquad (4)$$

Therefore, the phase difference maps contain information about the in-plane (Ly) and the out-of-plane (Lz) displacement. Once Ly is known, Lz can be obtained.

EXPERIMENTAL SET-UP A High Speed two-cavity New Wave Pegasus laser (λ = 527 nm, energy per pulse = 10 mJ at 1000 Hz) was used as a light source (figure 1). Two high speed cameras (Fastcam SA2, sensor size of 2048x2048 pixels, pixel size of 11 μm x 11 μm), were used to record the holograms (C1) and the PIV images (C2). The cameras were working at its maximum full size recording rate: 1000 images/s. Each laser was fired at half this rate (500 pulses/s). Two identical lenses (f'= 55 mm) have been used to image the illuminated fluid plane into both sensors with a magnification close to unity (M= 0.935). The lenses were working at f# = 22.

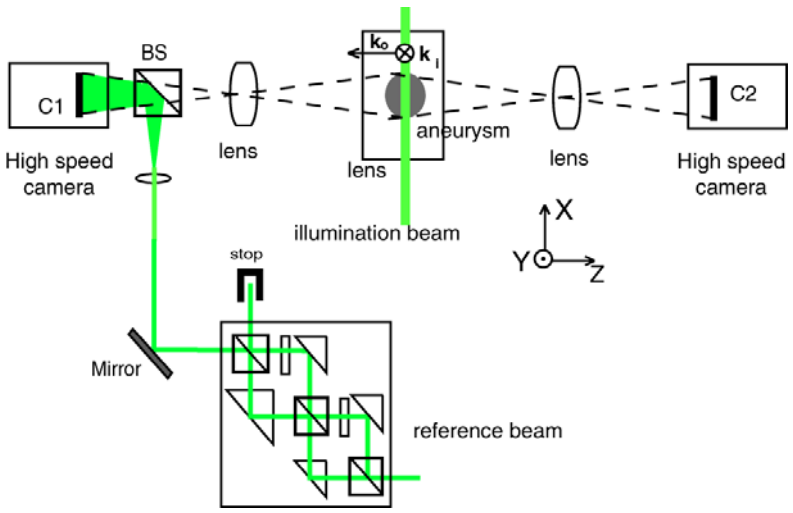

Fig. 1 Experimental set-up, top view

The laser beam is divided in the reference and illumination beam. The illumination beam is shaped into a sheet that illuminates the central plane of the aneurysm model, from above. The reference beam is splitted in four references with increasing optical paths using a compact and portable system. This system is needed due to the short laser coherence length (Lc ~ 10 mm in air, Lc/n_i in a fluid with refractive index n_i) which limits the length of the region that can be recorded. The 'apparent' coherence length of the reference beam is increased by overlapping several reference beams with controlled differences in their optical path lengths. Each beam will interfere with a different part of the object, whose length is the same as the laser coherence length. A detailed description of this part of the experimental set-up can be found in [9].

The brain aneurysm model is shown in figure 2 a. The model was built in very thin soft silicone which made it very flexible. It is a balloon of approximately 15 mm in diameter. The liquid that fills the model was chosen in order to match the silicon refractive index (refractive index n = 1.4185) and to have similar characteristics than blood (density

and viscosity). The best compromise is achieved with a mixture of water (n = 1.33) and glycerin (n=1.4734) in a ratio of 2/3 in weight. The liquid was seeded with 4-7 μm latex particles. The aneurysm model was immersed in a rectangular glass cell filled with the same liquid than the aneurysm for avoiding reflections from the model external walls.

This experimental set up was also used to measure the flow field in the central plane of a vein model with an antithrombotic filter inside (figure 2 b). The vein model was a piece of silicone tube (12 mm in internal diameter). The filter was located in the middle of the vein. Only camera 1 was used to record PIV images.

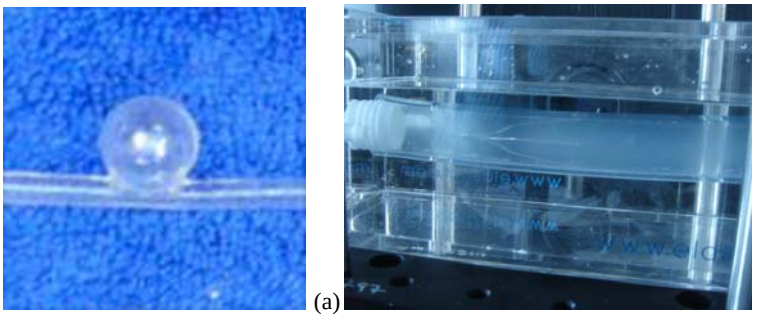

(a) (b)

Fig. 2 a) Brain aneurism model; b) vein model with the antithrombotic filter inside

RESULTS OBTAINED WITH THE ANEURISM MODEL The brain aneurism model was initially connected to a diaphragm pump in a closed circuit. A shock absorber was connected to the rubber pipes to remove the vibrations produced by the pump. The flow rate could be controlled by changing the voltage that feeds the pump. The flow rate, as measured with an ultrasonic base flowmeter, was set at 350 ml/min.

Camera 1 recorded holograms (figure 3a). Camera 2 recorded simultaneously PIV images (figure 3b). The background observed in the hologram is the reference beam. The pulse sequence is shown in the figure 4. With the pulses nA and nB a double exposure hologram is recorded in camera 1. The phase difference map (shown at the bottom of the image) is obtained from them. The images recorded with camera 2 with the pulses nA and nB allow the measurement of the displacement in the aneurysm main vessel, where the velocity is much higher than in the aneurysm balloon. The displacement field in the balloon is obtained from the images nA and (n+1)A.

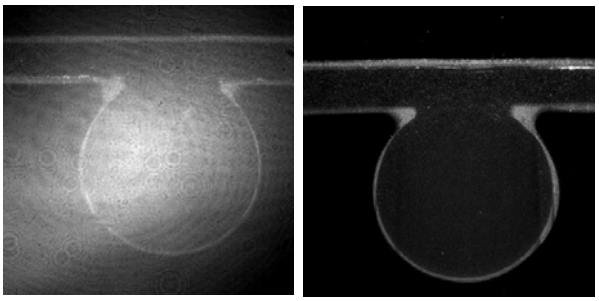

(a) (b)

Fig. 3 Brain aneurysm model as seen from each camera, a) hologram; b) PIV image

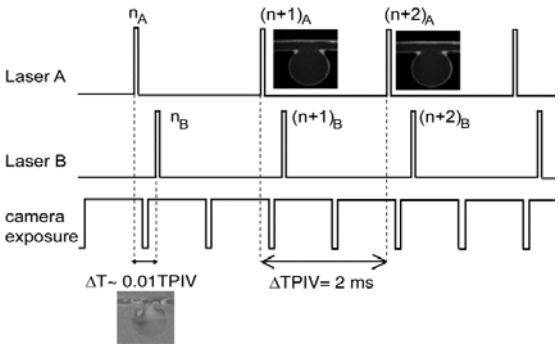

Fig. 4 Pulse sequence for the recording of the PIV images and holograms.

Series of hundreds of image pairs with different ΔT (5, 10, 25…μs) between the pulses nA and nB and of ΔTPIV= 2 ms between nA and (n+1)A, were recorded.

PIV images from camera 2 were analyzed using the Davis software from LaVision. The option of PIV sum of correlations was selected. This feature is convenient when the fluid seeding is sparse, as the final displacement vector is calculated by adding the cross-correlation peak in the same interrogation window (iw) in the whole image series. The velocity map was obtained in two steps. In the first one the iw size was 64 pixels and the overlapping between consecutive ones was 50%. In the second step the iw size was reduced to 32 pixels with a 50% of overlapping.

The holograms were analyzed using the interferometric approach explained before, so that phase difference maps which contain information about the out-of-plane velocity component were obtained. Due to the low seeding density the interference fringes present some discontinuities, that prevent is some cases a correct analysis of the phase maps. The fringe quality was improved by adding several phase difference maps. Figure 5 shows the sum of the phase difference maps from holograms recorded with $\Delta T = 5\ \mu s$.

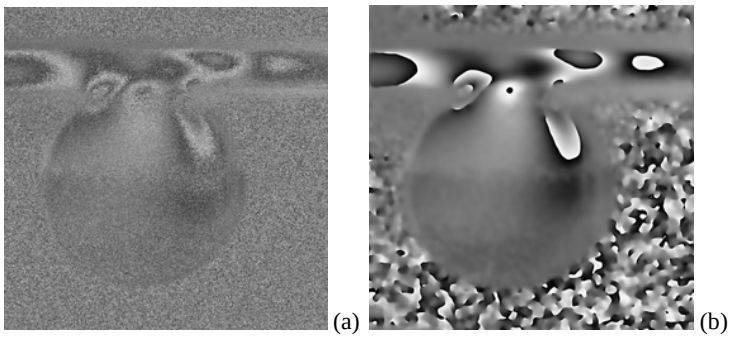
(a) (b)

Fig. 5: Phase difference maps, a) unfiltered; b) filtered

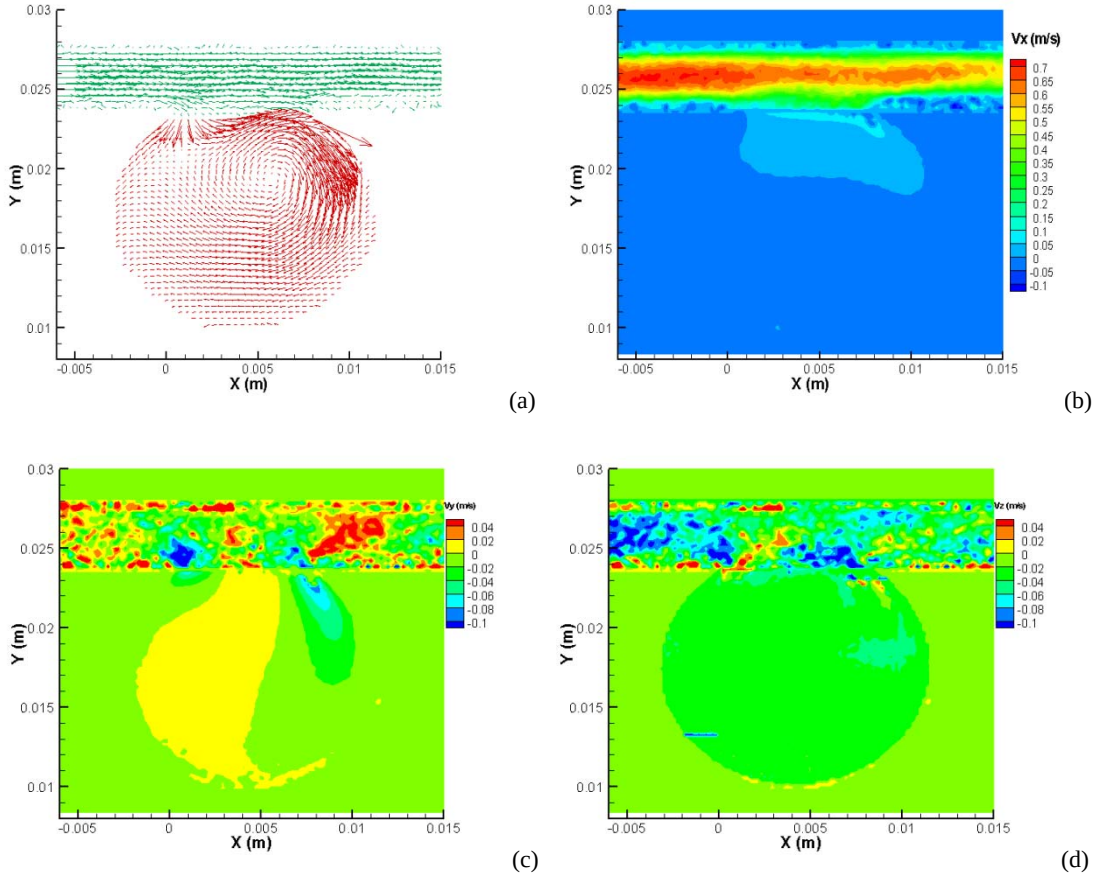

Fig. 6 Velocity fields measurements in the aneurysm; a) velocity vector map, b) Vx, b)Vy, d) Vz.

Figure 6 shows the complete velocity field. It can be seen that Vx is one order of magnitude bigger than Vy and Vz and is much higher in the vessel than in the balloon, as it was expected. Vy and Vz are of the same order of magnitude. In the aneurysm balloon, the contribution of the out-of plane component is practically zero. Figure 6a shows the velocity vector map. The values in the balloon (brown vectors) have been scaled by a factor of 20 in order to improve the flow structure visualization.

An interesting feature found in these measurements was some interference fringes that were obtained in the aneurysm wall. These fringes indicate changes in the wall shape which are due to small dilatations of the aneurysm. Figure 7 shows two examples of phase difference maps from a series of holograms recorded with ΔT= 100 μs. These maps were calculated from pairs of holograms recorded at different times. It was found that these fringe patterns repeated themselves with a frequency of 25 Hz.

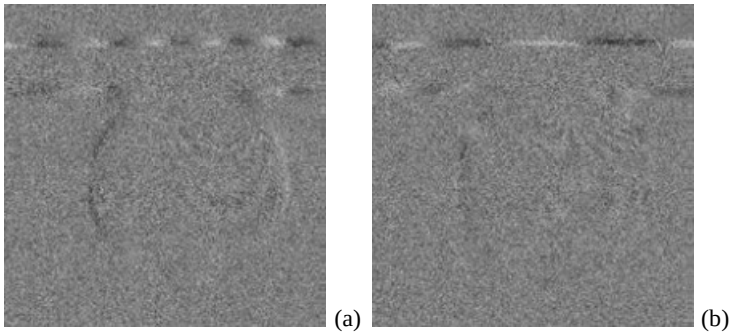

(a) (b)

Fig.7 Phase difference maps for ΔT= 100 μs, taken at different times; a) t = 2ms; b) t= 14 ms.

This change in the wall shape was somehow unexpected. A piston pump was used to find out if the aneurysm dilatation was due to the flow itself or to the pump. This pump is controlled by a PC and allows the use of physiological waves. In this case the flow rate was constant and set at 300 ml/min. No change in the wall shape was detected (figure 8). Therefore we concluded that changes in the pressure induced by the previous pump were causing the dilatation of the aneurysm. The velocity measurements obtained with the piston pump were very similar to velocities measured with the diaphragm pump.

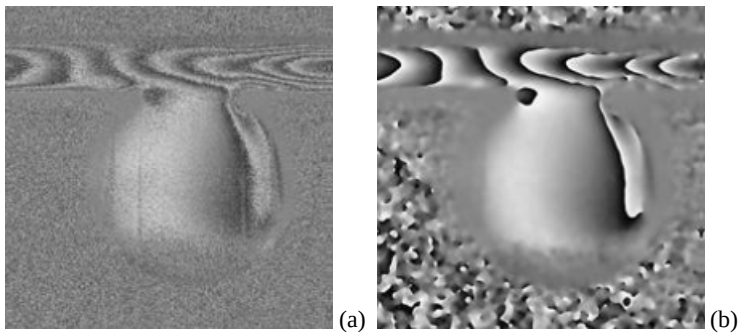

(a) (b)

Fig. 8 Phase difference maps, a) unfiltered; b) filtered

RESULTS OBTAINED WITH THE VEIN AND THE ANTITROMBOTIC FILTER A new numerical tool is being developed for the design of new antithrombotic filters. In order to validate the first stages of this tool, the experimental velocity was measured in model the vein with an antithrombotic filter inside. PIV images were recorded at 1000 Hz and analyzed using the Davis software from LaVision.

CFD was used together with the flow visualization to provide details on the effects of filters on the flow field. The filter and vena cava geometries were calculated using the Rhinoceros software. The vena cava vas modeled as a perfect cylinder with rigid walls and the filter was set in the vein centre. The numerical mesh was created using the ANSYS

ICEM CFD software. The mesh was built with tetrahedral elements. In the areas where more accuracy is needed, as the contact zone between the barbs and the vein walls, the mesh density is bigger. In the input and output flow areas, the elements density is smaller in order to accelerate the calculation. The laminar, stationary flow in the model was calculated using the program ANSYS CFX. The fluid was considered incompressible and viscous, with a constant density of 1.07 g/cm^3 and a viscosity of 0.041 g/cm s.

Figure 9 (a) shows the numerical results, while figure 9 (b) shows the experimental data. The experimental velocity field has been measured in five partially overlapping regions for higher spatial resolution on measurements. Figure 9 (b) shows the combination of those five velocity fields. A clear deceleration of the flow is measured due to the presence of the filter. The agreement between numerical and experimental results is not yet fully satisfactory. Some parameters such as the elasticity of the walls or fluid properties are being considered for further development of the numerical tool.

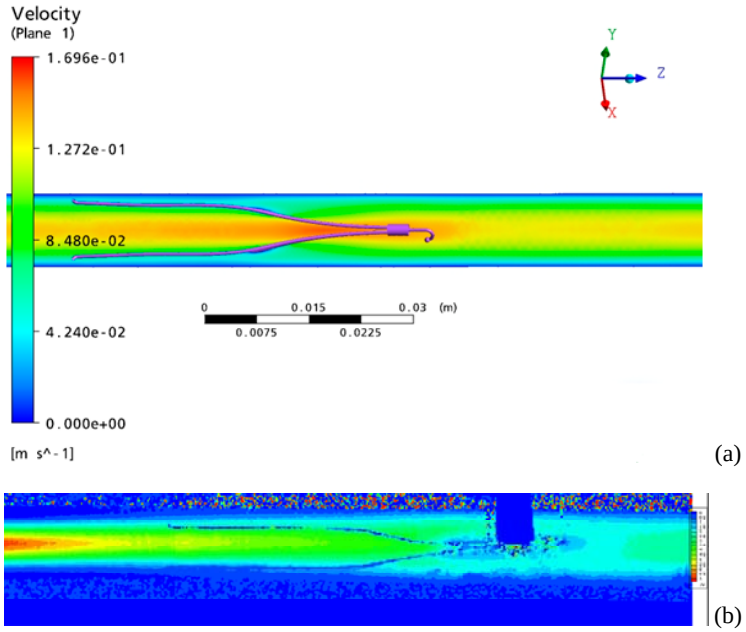

Fig. 9 a) Numerical simulation of the flow velocity in a vein with an antithrombotic filter inside. b) Experimental PIV results

CONCLUSIONS The complete velocity vector map has been obtained in a plane of a flexible brain aneurysm model using simultaneously high speed PIV and digital holography. PIV images provided the two in-plane velocity components. The phase difference maps obtained from the digital holograms provided not only the out-of-plane component but also information about the deformation produced, in specific conditions, in the model wall.

A new numerical code is being developed with the objective of designing new and more efficient antithrombotic filters. In order to validate this numerical tool, the velocity field in the central plane of a vein model with a filter inside has been measured with PIV. These experimental results have been compared with the numerical velocity field. From the comparison, it is clear that some parameters have to be careful controlled for the development of the numerical code.

References

1. Stehbens WE *Intracranial aneurysms*. In: Pathology of the Cerebral Blood Vessels, 1972, 51-470
2. Ferris E et al. *Percutaneous inferior vena caval filters: follow-up of seven designs in 320 patients*. Radiology 1993; 188(3):851-856
3. Gregorio MA et al. *Seguimiento clínico y por medios de imagen a largo plazo de los filtros de vena cava inferior. Estudio transversal*. Arch Bronconeumol 1995; 31(4):151-156.
4. Gregorio MA et al. *Animal experience in the Gunther Tulip retrievable inferior vena cava filter*. Cardiovasc Intervent Radiol 2001; 24: 413-417.
5. Raffel M et al. *Particle Image Velocimetry, a practical guide*. 1998. Springer Verlag
6. Burke J et al. *Digital holography for whole field spray diagnostic*, In: Proceedings of the 11th international symposium on applications of laser techniques to fluids mechanics, Portugal, 2002, paper 10.1
7. Lobera J et al. *Digital speckle pattern interferometry as a holographic velocimetry technique*. Measurement Science and Technology, 2004, 15:718–724
8. Arroyo MP, et a. *Digital Image Plane Holography for Three-Component Velocity Measurements in Turbomachinery Flows*, In: Proceedings of the 13 th Int Symp on Applicatons of Laser Techniques to Fluid Mechanics, Portugal, 2006
9. Palero V. et al. *Three Component Velocity Field Measurement in Confined Liquid Flows with High Speed Digital Image Plane Holography*. Exp. Fluids 2010, **49**, p 471-483
10. Vest CM *Holographic interferometry*, 1979 Wiley Series in Pure and Applied Optics. Wiley, New Yor